http://dx.doi.org/10.5012/bkcs.2013.34.1.321

Synthesis of a White-Light-Emitting ZnSe:Mn Nanocrystal *via* Thermal Decomposition Reaction of Organometallic Precursors

Sang-Min Lee and Cheong-Soo Hwang*

Department of Chemistry, Institute of Nanosensor and Biotechnology, Dankook University, Gyonggi-Do 448-701, Korea
**E-mail: cshwang@dankook.ac.kr*
Received August 1, 2012, Accepted August 31, 2012

Key Words : ZnSe:Mn nanocrystal, White light emission, Semiconductor nanocrystal, Photoluminescence

Low-dimensional nanosized semiconductor materials, such as quantum dots, have attracted considerable interest in the past decade.[1,2] Due to their size-dependent physical and optical properties, these nanosized semiconductor materials offer various technological applications in photoelectronic devices.[3-5] Among the II-VI semiconductor materials, zinc selenide (ZnSe) is of special interest due to its intense UV blue light emission at 460 nm wavelength with a band gap of 2.7 eV, which has not been observed in other well-known semiconductor materials, such as CdS and CdSe.[6-9] In addition, it has been reported that when the surface of ZnSe is passivated by another semiconductor nanocrystal layer such as ZnS, a ZnSe/ZnS core shell quantum dot can be formed, and the quantum yield of the ZnSe/ZnS quantum dot is much higher (about 20 times) than that of bare ZnSe nanocrystallite.[10] The preparation method of ZnSe or ZnSe/ZnS quantum dot often includes a thermal decomposition reaction of organometallic precursors in a hot coordinating organic solvent such as trioctylphosphineoxide (TOPO), leading to a hydrophobic surface on the resulting nanocrystal. Previously, in this lab, water-dispersible ZnSe and ZnSe/ZnS nanocrystals were also prepared by exchanging the hydrophobic nanocrystal surface with polar organic ligands such as mercaptoacetic acid (MAA) and ethylenediaminetetraacetic acid (EDTA) molecules.[11,12]

Manganese-ion doped ZnSe nanocrystals have been prepared in various media. In most cases, emission wavelengths of the ZnSe:Mn nanocrystals were far shifted from that of the undoped ZnSe nanocrystal. They usually emit orange-colored lights (580-600 nm) due to the dopant Mn ions.[13,14] In this paper we report on the synthesis of Mn^{2+} ion-doped ZnSe nanocrystal *via* thermal decomposition reaction from organometallic precursors, and unexpected white light emission from the prepared ZnSe:Mn nanocrystal.

Figure 1 presents an HR-TEM image of ZnSe:Mn nanocrystal. In the picture, the measured and calculated average particle size was 3.5 nm. In addition, the appearance of distinct lattice planes in the fringe image with an approximate spacing of 3.4 Å suggests that all the solid samples were made of single crystals rather than poly-crystalline aggregate mixtures.

An energy dispersive X-ray spectroscopy diagram (EDXS, in Fig. 2) was also obtained to confirm the elemental compositions of the ZnSe:Mn nanocrystal in the solid state. The obtained doping concentration of manganese(II) ions in the ZnSe:Mn nanocrystal was 2.3 atomic %. To determine the doping concentration of Mn^{2+} ions more precisely, Inductively Coupled Plasma-Atomic Emission Spectrometry (ICP-AES) analysis was performed. Three trials of the sample measurements revealed that the average elemental proportion of the Mn^{2+} ions relative to ZnSe parent crystal was

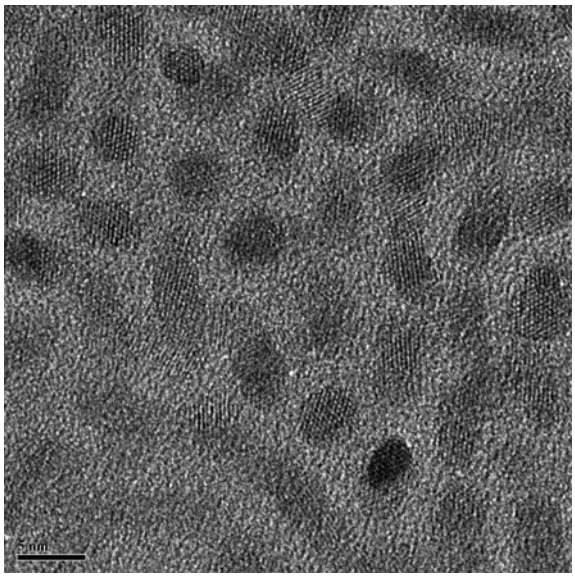

Figure 1. HR-TEM image of ZnSe:Mn nanocrystal, the scale bar represents 5 nm.

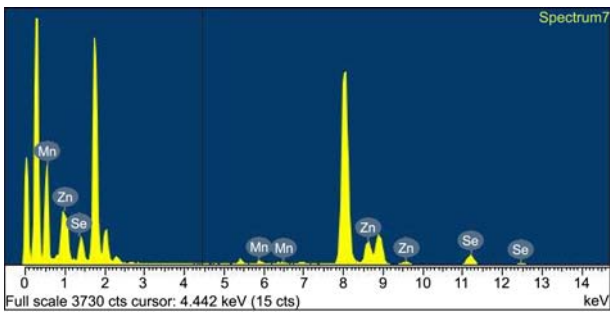

Figure 2. Energy dispersive X-ray spectroscopy (EDXS) diagram of ZnSe:Mn nanocrystal.

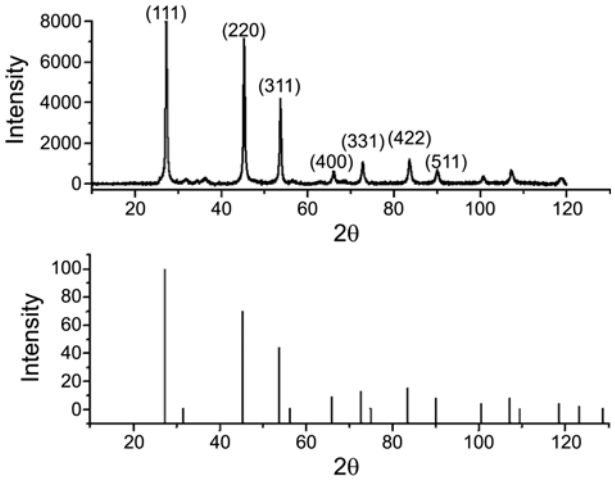

Figure 3. X-ray diffraction pattern diagrams of ZnSe:Mn nanocrystal (top) and bulk ZnSe solid in a cubic Stilleite phase (bottom).

2.83%, which showed good agreement with the result obtained from the EDXS analysis.

As shown in Figure 3, a wide-angle x-ray diffraction pattern diagram of the ZnSe:Mn nanocrystalline powder was obtained to confirm the formation of ZnSe parent crystal lattice. In the diffraction pattern diagram, the apparent peaks at (111), (220), (311), (400), (331), (422) and (511) planes for the ZnSe:Mn powder sample are identical to that for the reported bulk ZnSe solid in a cubic Stilleite crystalline phase (JCPDS 37-1463). In addition, we also performed Debye-Scherrer calculations for ZnSe:Mn nanocrystal by using the obtained XRD peaks to compare to the particle size measured from the HR-TEM image.[15,16] As a result, our calculation revealed that the average particle size for ZnSe:Mn particles was 4.2 nm, which was similar to that obtained from the HR-TEM image.

Figures 4(a) and (b) present absorption and emission spectra of ZnSe:Mn nanocrystal. The UV-vis absorption spectrum (Fig. 4(a)) showed a broad absorption peak at 271 nm, with a small shoulder at 277 nm. The room-temperature solution PL spectrum (Fig. 4(b)) revealed two broad emission peaks at 445 and 572 nm, respectively. The dominant absorption shown in the UV-vis spectrum is probably caused by the fundamental band-to-band absorption in the ZnSe host,[17] and the increased band gap compared to bulk ZnSe solid (2.7 eV) is due to the quantum confinement effect for nanosize materials.[18] The emission spectrum was obtained by fixing the excitation wavelengths of the light source at the maximum absorption wavelength in the UV-visible spectrum. From the absorption and emission spectra, one can see a large Stokes shift of *ca.* 168 nm for the ZnSe:Mn nanocrystal. The large Stokes shift in the absorption-emission energy gap difference can be described as a characteristic of zero-dimensional nanocrystals, which is usually due to the presence of traps originating from surface levels and other intrinsic defects.[19] The surface defect on the ZnSe:Mn nanocrystal probably resulted from incomplete capping by the surfactant TOPO ligands, or from the zinc metal cation or selenide

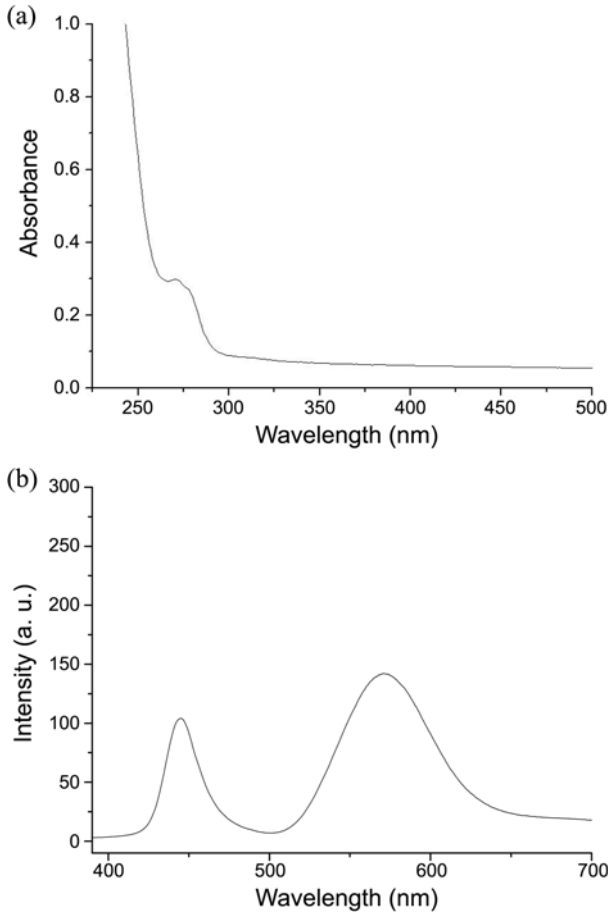

Figure 4. (a) UV-visible absorption spectrum of ZnSe:Mn nanocrystal. (b) Room-temperature photoluminescence spectrum of ZnSe:Mn nanocrystal (dispersed in hexane).

anion vacancy on the surface of the crystal lattice. In the ZnSe:Mn nanocrystal, the orange light emission at 572 nm is attributed to the $^4T_1 - {}^6A_1$ transition of Mn^{2+} ions.[20] In the luminescence pathway, if the surface defect states are located close to the conduction band, direct energy transfer from the ZnSe host to the Mn^{2+} dopant ion is significantly interrupted, which can cause weakening in the orange emission as well as enlarging the Stokes shift.[21]

White light emission from a manganese-ion-doped semiconductor nanocrystal has been observed in ZnS:Mn nanocrystal capped with 8-hydroxyquinoline-5-sulfonic acid (HQS).[22] ZnS:Mn-HQS NC was prepared in aqueous solution from the reaction of zinc nitrate, sodium sulfide, and manganese(II) acetate under reflux conditions. The optimized Mn ion doping concentration was 2%, which is close to that for our ZnSe:Mn nanocrystal. The ZnS:Mn-HQS showed two emission PL peaks at 475 nm (blue) and 600 nm (yellow-orange) wavelengths. The emission peak that appeared at 600 nm was assigned to $^4T_1 - {}^6A_1$ transition for the dopant Mn^{2+} ions, and the blue emission at 475 nm was described as a result of the incomplete energy transfer between the ZnS lattice and the dopant ion due to the presence of both interstitials and vacancies of zinc or sulfide ions in the ZnS lattice.[23] We believe the same phenomenon occurred

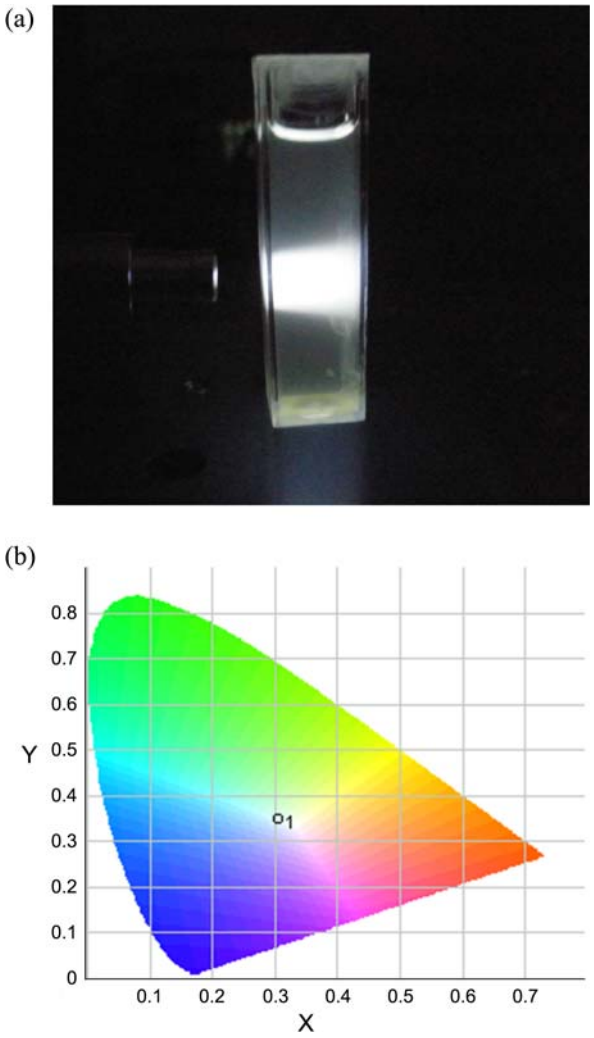

Figure 5. (a) A light scattering picture of ZnSe:Mn nanocrystal exposed to He-Cd laser (325 nm) light. (b) CIE Chromaticity diagram of ZnSe:Mn nanocrystal (O_1 stands the position of the ZnSe:Mn nanocrystal powder sample).

in our ZnSe:Mn nanocrystal. Combining the two complementary emissions from the ZnS:Mn and our ZnSe:Mn nanocrystals afforded the resulting white light

The PL efficiencies for the ZnSe:Mn nanocrystal was measured and calculated by following the same method reported by Williams *et al.*[24] to calculate the relative quantum yield by comparing to a standard material in the literature,[25] 0.1 M solution of quinine sulfate in H_2SO_4 (Fluka) in our case, whose emission wavelength and reported absolute quantum yield are 550-600 nm and 0.546 (at 22 °C), respectively. The excitation wavelength used for the standard (quinine sulfate) solution was obtained from the UV-vis spectrum for the ZnSe:Mn nanocrystal. In the calculation, a total integrated fluorescence area was taken as the sum of each integrated area of the two emission peaks, and a refractive index for the solvent was also corrected for hexane (1.37 at 20 °C). As a result, the calculated relative PL efficiency for the white-light-emitting ZnSe:Mn nanocrystal was 11.8% compared against the standard material.

In Figure 5(a), the presented light scattering picture was taken by exposing the ZnSe:Mn nanocrystal containing hexane solution to 325 nm He/Cd laser light whose emission wavelength is close to the excitation wavelengths of the ZnSe:Mn nanocrystal. The picture shows white light emission from the ZnSe:Mn nanocrystal containing pale-yellow hexane solution, with a characteristic bright light scattering of a nanoparticle dispersed colloidal solution. Finally, Figure 5(b) shows a CIE chromaticity diagram of the ZnSe:Mn nanocrystal. The obtained color coordinate was (x = 0.32, y = 0.34) for the ZnSe:Mn nanocrystal powder sample. For the ZnS:Mn nanocrystal, the measured color coordinate was somewhat changed by varying the concentration of the Mn dopant; however, we did not observe such changes in our ZnSe:Mn nanocrystal.

In summary, we have synthesized white-light-emitting ZnSe:Mn nanocrystal *via* thermal decomposition reaction of diethyl zinc, manganese(II) cyclohexabutylate, and elemental selenium dispersed in TOP solvent. The obtained ZnSe:Mn nanocrystal was optically characterized by UV-vis and room-temperature solution PL spectroscopy. The further obtained powder was characterized by XRD, HR-TEM, EDXS, and ICP-AES analyses. The solution PL spectra showed two broad emission peaks at 445 and 572 nm, and light is produced by combining those complementary color emissions. In this lab, further application studies such as fabrication of electronic illumination devices like LEDs using the ZnSe:Mn nanocrystal are in progress.

Experimental Section

Chemicals and Instruments. All the solvents used in this experiment were purchased from Aldrich and distilled before use. Diethylzinc (0.1 M solution in hexane), hexadecylamine (HDA, 90%), tri-*n*-octylphosphine (TOP, 90%), manganese (II) cyclohexabutylate and Selenium powder (~100 mesh 99.999%) were purchased from Aldrich and used as received. 1 M (TOP)Se stock solution was prepared in a dry box *via* mixing of 0.78 g (0.01 mol) of Se powder with TOP solvent so that the total volume of the solution reached 10 mL in a volumetric flask. The UV-vis absorption spectrum was recorded on a Perkin Elmer Lambda 25 spectrophotometer equipped with a deuterium/tungsten lamp. The solution photoluminescence spectra were taken by a Perkin Elmer LS-45 spectrophotometer equipped with a 500 W Xenon lamp, a 0.275-m triple grating monochrometer, and a PHV 400 photomultiplier tube. HR-TEM images were taken with a JEOL JEM 1210 electron microscope with a MAG mode of 1000 to 800000, and the accelerating voltage was 40-120 kV. The samples for the TEM were prepared *via* dispersion into methanol solvent and placement on a carbon-coated copper grid (300 Mesh), followed by drying under vacuum. In addition, the elemental compositions of the nanocrystals were determined by EDXS (Energy Dispersive X-ray Spectroscopy) spectra, which were obtained *via* an EDXS collecting unit equipped in the HR-TEM, with a Si (Li) detector in an IXRF 500 system. ICP-AES elemental

analyses were performed by Optima-430 (Perkin Elmer) spectrometer equipped with an Echelle optics system and a segmented-array charge-coupled device (SCD) detector. Finally, the provided light scattering picture of the nanocrystal containing colloid was taken by exposure of KIMMON IK3202-R He-Cd laser (325.0 nm) light.

Synthesis of the ZnSe:Mn Nanocrystal. The preparation method was modified slightly from the method previously reported in the literature.[11] All the manipulations were carried out using modified Schlenk techniques under an inert atmosphere of Argon. 50 mL of HDA solvent were placed in a 200 mL three-neck flask connected to a vacuum manifold. The liquid was dried and degassed under vacuum at *ca*. 125 °C for 7 h, and then the flask was filled with argon gas. A 10 mL solution of manganese(II) cyclohexabutylate (0.04 mmol) dissolved in TOPO was injected into the flask containing HDA. 2.0 mL of separately prepared 1 M TOPSe stock solution was taken out with a glass syringe from the dry box, and immediately transferred to the flask containing the hot HDA solvent. Further addition of 20 mL of 0.1 M Et_2Zn (2.0 mmol) solution was carried out at 300 °C. After mixing the precursors, a vigorous reaction occurred immediately, and the mixture was stirred for 30 minutes. The mixture solution was cooled to 90 °C and incubated for 10 hours at this temperature. Further cooling to ambient temperature and the addition of anhydrous ethanol resulted in the formation of pale yellow precipitate. The isolated ZnSe:Mn nanocrystal powder, which was produced by multiple centrifuging and filtering, was redispersed in 50 mL of anhydrous hexane solvent.

Acknowledgments. The present research was supported by the Research Fund of Dankook University in 2010.

References

1. Murray, C. B.; Norris, D. J.; Bawendi, M. G. *J. Am. Chem. Soc*. **1993**, *115*, 8706.
2. Alivisatos, P. *J. Phys. Chem*. **1996**, *100*, 13226.
3. Heath, J. R. *Acc. Chem. Res*. **1999**, 3.
4. Jaiswal, J. K.; Mattoussi, H.; Mauro, J. M.; Simon, S. M. *Nature Biotechnol*. **2002**, *21*, 47.
5. Milliron, D. J.; Alivisatos, A. P.; Pitois, C.; Edder, C.; Frechet, J. M. *J. Adv. Mater*. **2003**, *15*, 58.
6. Chestnoy, N.; Hull, R.; Brus, L. E. *J. Chem. Phys*. **1986**, *85*, 2237.
7. Hines, M. A.; Guyot-Sionnest, P. *J. Phys. Chem. B* **1998**, *102*, 3655.
8. Revaprasadu, N.; Malik, M. A.; O'Brien, P. *J. Mater. Chem*. **1998**, *8*, 1885.
9. Dey, S. C.; Nath, S. S. *J. Lumin.* **2011**, *131*, 2707.
10. Song, K. K.; Lee, S. H. *Curr. Appl. Phys*. **2001**, *1*, 169.
11. Hwang, C.-S.; Cho, I. H. *Bull. Kor. Chem. Soc*. **2005**, *26*, 1776.
12. Lee, J. W.; Lee, S. M.; Huh, Y. D.; Hwang, C.-S. *Bull. Kor. Chem. Soc*. **2010**, *31*, 1997.
13. Suyver, J. F.; Wuister, S. F.; Kelly, J. J.; Meijerink, A. *Phys. Chem. Chem. Phys.* **2000**, *2*, 5445.
14. Fang, Z.; Wu, P.; Zhong, X.; Yang, Y. J. *Nanotech.* **2010**, *21*, 305604.
15. International Union of Crystallography in International Tables for X-Ray Crystallography, Part III; Netherlands, Dordrecht, 1985; p 318.
16. Qinghong, Z.; Lian, G.; Jinkun, G. *Appl. Catal. B Environ.* **2000**, *26*, 207.
17. Hasse, M. A.; Qui, J.; DePuydt, J. M.; Cheng, H. *Appl. Phys. Lett.* **1991**, *59*, 1272.
18. Lippens, P. E.; Lannoo, M. *Phys. Rev. B* **1989**, *39*, 10935.
19. Kumbhokjar, N.; Mahamuni, S.; Leppert, V.; Risbud, S. H. *Nanostruc. Mater.* **1998**, *10*, 117.
20. Chen, W.; Su, F.; Li, G.; Joly, A. G.; Malm, J.-O.; Bovin, J.-O. *J. Appl. Phys.* **2002**, *92*, 1950.
21. Dong, B.; Cao, L.; Su, G.; Liu, W.; Zhai, H. *J. Alloys and Comp.* **2010**, *429*, 363.
22. Lü, X.; Yang, J.; Fu, Y.; Liu, Q.; Qi, B.; Lü, C.; Su, Z. *Nanotech.* **2010**, *21*, 115702.
23. Sarkar, R.; Tiwary, C. S.; Kumbhakar, P.; Basu, S.; Mitra, A. K. *Physica E* **2008**, *40*, 3115.
24. Williams, A. T. R.; Winfield, S. A.; Miller, J. N. *Analyst*. **1983**, *108*, 1067.
25. Melhuish, W. H. *J. Phys. Chem*. **1961**, *65*, 229.